International Journal of Thermodynamics (IJoT)
ISSN 1301-9724 / e-ISSN 2146-1511
www.ijoticat.com

Vol. 14 (No. 3), pp. 97-105, 2011
doi: 10.5541/ijot.296
Published online: May 25, 2011

Thermodynamic Justification for the Ni/Al/Ni Joint Formation by Diffusion Brazing

W. S. Wołczyński*[1], T. Okane[2], C. Senderowski[3], D. Zasada[3], B. Kania[4], J. Janczak-Rusch[5]

[1]Institute of Metallurgy & Materials Science, Polish Academy of Sciences, Reymonta 25, 30 059 Kraków, Poland
[2] AIST – National Institute of Advanced Industrial Science & Technology, Umezono 1-1-1, 305 8568 Tsukuba, Japan
[3]Military University of Technology, Kaliskiego 2, 00-908 Warszawa, Poland
[4]AGH – University of Science & Technology, Reymonta 19, 30-059 Kraków, Poland
[5]EMPA–Swiss Federal Laboratories for Materials Science & Technology, Ueberland 129, 86 000 Duebendorf, Switzerland
*nmwolczy@imim-pan.krakow.pl

Abstract

A theoretical model for the joint formation was developed for diffusion brazing. The phenomena of dissolution and solidification were included into the model. A thermodynamic justification for the isothermal brazing occurrence in the meta-stable conditions was developed. It involved the application of the criterion of higher temperature of the solid / liquid (s/l) interface. The dissolution of the filler metal in the substrate was described by the N_0 – solute concentration within the dissolution zone (liquid film) situated at the substrate surface. The selection of the N_0 – parameter was justified by the Thermocalc calculation of the Ni-Al phase diagram for meta-stable equilibrium. According to the model assumptions, the solidification was accompanied by undercooled peritectic reactions resulting in formation of intermetallic phases. The average Al – solute concentration measured across a given $Al_3Ni_2/Al_3Ni/Al_3Ni_2$ joint confirmed that the N_0 – solute concentration was conserved within the joint sub-layers. The Ni-Al phase diagram for meta-stable equilibrium referred to for the solidification was also calculated by means of the *Thermocalc Software*. It allowed to locate the solidification path, s/l interface path and redistribution path onto the mentioned diagram. Superposition of both calculated phase diagrams was also given to show that the joint formation occurred cyclically under the meta-stable conditions. Isothermal formation of the Ni/Al/Ni joints has been performed at different temperatures. The following T_R – temperatures have been applied: 700, 750, 800, 850, 900, 950, and 1000 ^{0}C. The solidification was arrested and the actual morphologies frozen. It allowed to make a measurement of the Al - solute concentration across each joint by means of the EDX micro-analyzer to estimate average solute concentration, $\overline{N}_0$. Regardless of the T_R - temperature, the solidification path was always the same.

Keywords: *: meta-stable equilibrium, joint formation model, dissolution, solidification*

1. Introduction

A solidification, a dissolution and some solid/solid transformations are predicted by Tuah-Poku et al., (1988) as phenomena which are to be observed during diffusion brazing.

The solidification and dissolution are subjected to consideration in the current model. However, exceptionally the first solid / solid transformation is strictly connected with solidification and dissolution through the mass balance (Kloch et al., 2005).

A dissolution of substrate by the liquid filler metal occurs continuously within a zone dx, Figure 1. The dissolution prepares the liquid film within the zone dx. Once the zone becomes liquid the mass of this liquid film diffuses towards the joint symmetry axis and solidification occurs at the s/l interfaces, (Wołczyński et al., 2006a).

Solidification is accompanied by the undercooled peritectic reactions, Figure 2. According to the concept of Chuang et al. (1975), undercooled peritectic reactions take place at the solid/liquid (s/l) interface.

The occurrence of peritectic reactions at the s/l interface of cells formed within a given sub-layer are marked schematically with some arrows in Figure 2.

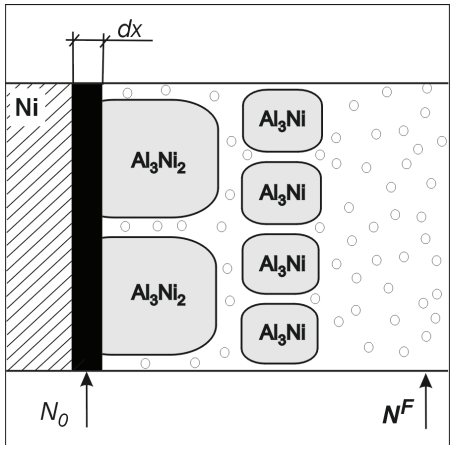

Figure 1. Ni-substrate dissolution within its infinitesimally small amount, dx (the so-called zone dx situated just at the substrate surface) due to diffusion of liquid solution of the filler metal, N^F, through the channels situated among some cells of Al_3Ni_2 or Al_3Ni phases formed in a given sub-layer, respectively. A reaction within the zone is as follows: $liquid(N^F) + Ni \rightarrow undercooled\ liquid\ (N_0)$.

The internal channels within cells are mainly employed for the flow of dissolved substrate towards the s/l interfaces (bulk diffusion). The dissolved substrate contained within zone dx has the solute concentration equal to N_0, Figure 1.

Under the described conditions, a bonding process can result in a joint that reproduces micro-structurally a sequence of inter-metallic compounds or phases as it is visible in an adequate phase diagram for stable equilibrium, (Jacobson and Humpston, 1992; Wołczyński et al., 2006b).

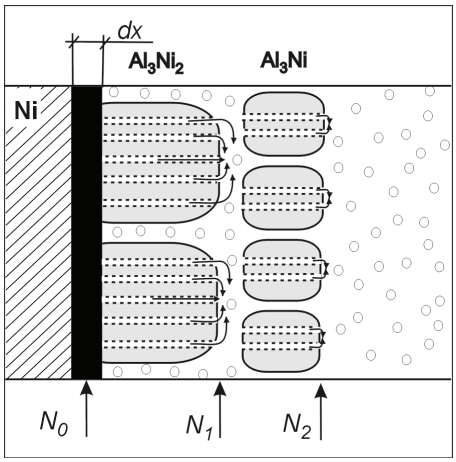

Figure 2. The undercooled peritectic reactions at the front of cells (as it results from the phase diagram for stable equilibrium): N_1 – solute concentration within undercooled liquid for the first peritectic reaction resulting in formation of the sub-layer that contains cells of the Al_3Ni_2 intermetallic phase, N_2 – solute concentration within undercooled liquid for the second peritectic reaction resulting in formation of the sub-layer that contains cells of the Al_3Ni intermetallic compound. The channels predicted in the model for bulk diffusion are shown schematically and completed with some arrows that signify occurrence of a given peritectic reaction.

The analysis is focused on the formation of the Ni/Al/Ni joints in relation to the diffusion brazing. It makes it possible to develop a description for the solidification preceded by the dissolution and a new explanation for the role of the solidification path for the creation of the joint sub-layers.

Additionally, a thermodynamic justification for the beginning of solidification path, N_0 and the end of solidification path, N^F, are both given. The *Thermocalc* calculation of the Ni-Al phase diagram for meta-stable equilibrium will give the grounds for this justification.

2. Solidification / dissolution model for the formation $NiAl_3Ni_2/Al_3Ni/Al_3Ni_2$-Ni joint

The system selects one and only one nominal concentration of the solute, N_0 at a given temperature, T_R, (Kloch et al., 2005). The selection of the N_0 - parameter by the system occurs in such a way to ensure the film, dx (zone dx), to be liquid. The zone dx is created at the surface of a substrate, Figure 1. It is evident that the liquid layer, dx, is strongly undercooled from its *liquidus* temperature. Thus, dissolution occurs at a given temperature, T_R, as long as it is necessary to transform solid substrate zone, dx, into the liquid film, dx.

Once the dx zone becomes liquid and its concentration achieves a selected N_0, the undercooled liquid film is ready to be subjected to solidification involving undercooled meta-stable peritectic reactions, Figure 2.

The average Al-solute content measured within the Ni/Al/Ni joint obtained after different periods of time is always equal to the N_0 - concentration. Thus, the N_0 - parameter is situated on the *liquidus* line as the beginning of solidification path, Figure 3.

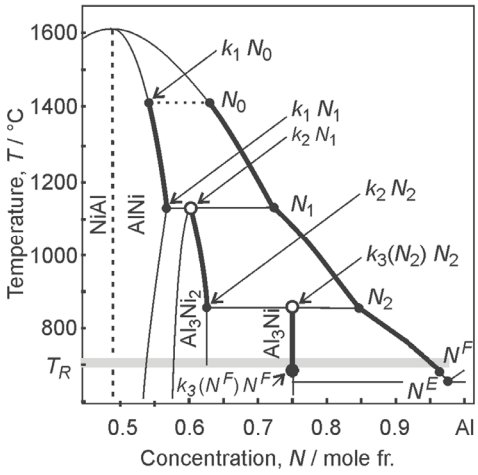

Figure 3. Ni-Al phase diagram for stable equilibrium with the $N_0 \rightarrow N_1 \rightarrow N_2 \rightarrow N^F$ solidification path and with the $k_1N_0 \rightarrow k_1N_1 \rightarrow k_2N_1 \rightarrow k_2N_2 \rightarrow k_3(N_2)N_2 \rightarrow k_3(N^F)N^F$ "historical" solid / liquid interface path. T_R = 700 ^{0}C, and N_0 = 0.64 [mole fr.].

According to the current model assumption, the constant partitioning is justified for the formation of an intermetallic phase. In the case of an inter-metallic compound formation a varying partition ratio is to be applied. Thus, the universal definition of the k – partition ratio was introduced:

$$k_i(N_i^L) = k_i^0 + k_i^L \; N_{i-1}/N_i^L \qquad 1, \ldots, n, \qquad (1)$$

As the assumed peritectic reaction $x_i + liquid\ (N_i) \rightarrow \left[x_i^{max} - x_i^{min}\right]$ occurs during solidification, the amount of the primary phase is to be defined accordingly.

$$x_i(\alpha_i^D, l_i^0, N_{i-1}, N_i, k_i) = l_i^0 \left[(1 - (N_i/N_{i-1})^{(1-\alpha_i^D\, k_i)/(k_i-1)})/(1 - \alpha_i^D\, k_i)\right] \quad (2)$$

Eq. (1) is universal and can be applied to the descriptions of a peritectic reaction when: a/ an intermetallic phase is formed, then $k_i^L = 0$; and, b/ an intermetallic compound is formed, then $k_i^L \neq 0$ and the use of Eq. (1) in its full form is recommended. The x_i^{max} and x_i^{min} - parameters have already been defined in detail, (Wołczyński et al., 2006a). Finally, the model allows determination of the ratio of sub-layers thickness, $\lambda_1^K/\lambda_2^K = x_1^{max}/(x_2^{max} + x_3)$, Figure 4, with some explanations shown in Figure 5.

According to the current model, the solute concentration within a given sub-layer should be the same as the solute concentration at the peritectic point in the phase diagram.

Thus, the Al solute concentration equals 60 at.%, for the Al_3Ni_2 – intermetallic phase and 75 at.% for the Al_3Ni – intermetallic compound.

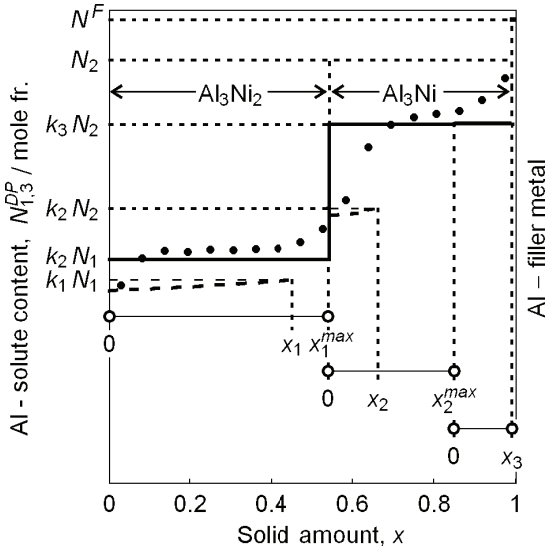

Figure 4. Reproduction of the sub-layers thickness ratio together with the measured solute redistribution profile (dots) resulting from the undercooled peritectic reactions. Profiles are mirrored across the centerline of the joint (dotted line): Ni / Al_3Ni_2 / Al_3Ni / Al_3Ni_2 / Ni. The ratio of sub-layers thickness is reproduced for the solidification path $N_0 \rightarrow N^F$ shown in Figure 3. The measurement points (dots) are taken from the EDX analysis. Solidification was carried out at 700 ^{0}C for 121 [s].

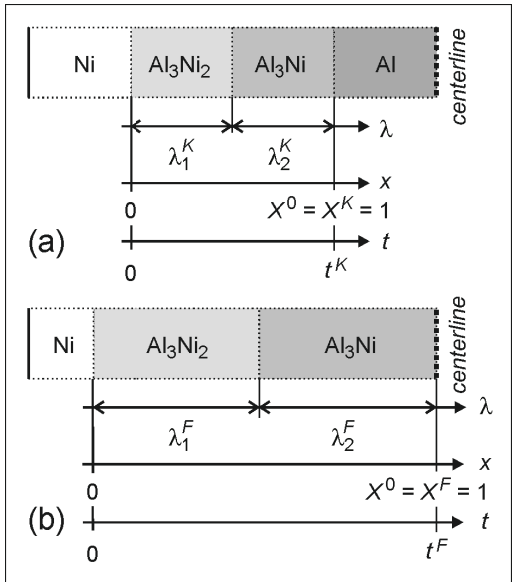

Figure 5. The meaning of some parameters in solidification of the Al_3Ni_2 /Al_3Ni multilayer on the Ni-substrate shown at: a/ a given step of the Al_3Ni_2 /Al_3Ni multi-layer formation; and, b/ completion of the Al_3Ni_2 /Al_3Ni multilayer formation.

Thus, it will be verified whether the ratio of sub-layers thickness depends on the real temperature, T_R, at which the experiment is performed.

3. Experimental verification of the current model for solidification/dissolution

A set of experiments was carried out in order to study the sequence of the intermetallic sub-layers formation. The experiment of the Ni/Al/Ni diffusion joint formation was performed at different temperatures: 700, 750, 800, 850, 900, 950 and 1000 ^{0}C.

An Al-foil 25 μm thick was located between two pieces of nickel then tightened. The Ni/Al/Ni system was put into a vacuum furnace, then heated until a given temperature.

At each of the imposed temperatures, the Al-foil was melted and the system subjected to dissolution / solidification. The solidification was halted after a given period of time and the morphology of the interconnections was frozen, Figure 6.

The Al-solute segregation profiles were analyzed across the frozen interconnections by means of the EDX – micro-analyzer. Next, an average content of the Al-solute, $\widehat{N}_0$, was determined for each of the studied joints. The estimated results are gathered in Table 1.

Since the values of the $\widehat{N}_0$ - parameter (Table 1) are similar to each other, the average Al - solute content, denoted as $\overline{N}_0$, and representative for all investigated joints was calculated. It is equal to $\overline{N}_0 \approx 0.64$ [mole fr.], ($\overline{N}_0 \cong (1/7)\sum \widehat{N}_0$).

The revealed interconnections morphology proved that the ratio of sub-layers thickness does not change with the T_R - temperature imposed in a given experiment. This conclusion does not result directly from the ratio of areas marked for sub-layers visible in Figure 6a., and Figure 6b.

It was necessary to correct the thickness of the Al_3Ni phase sub-layers as follows:

a/ in the case when the areas of the N^F solution exist inside the sub-layer, the thickness of the Al_3Ni phase sub-layers is to be diminished. The diminution is required since the N^F solution did not yet transform into the joint. It is clearly visible in Figure 6a.

b/ in the case, when the areas of the pure Al exist inside the sub-layer, the thickness of the Al_3Ni phase sub-layers is to be enlarged and the thickness of the Al_3Ni_2 phase sub-layer diminished adequately. It is required since the presence of pure Al located inside the Al_3Ni phase sub-layers is the product of the so-called "*mantis phenomenon*". The phenomenon is described by the reaction which is as follows: $2\,Al_3Ni \rightarrow Al_3Ni_2 + 3\,Al$.

It was evident that the above reaction (if it occurred) diminished slightly the Al_3Ni phase sub-layers and thickened a little the Al_3Ni_2 phase sub-layer. It is visible in Figure 6b.

Therefore, the adequate corrections were made while analyzing the ratio of thicknesses of both sub-layers.

It should be emphasized that according to the mass balance the average solute content, $\overline{N}_0$, revealed in the frozen interconnections is to be equal to the initial solute content, N_0, from which the interconnections were formed during solidification accompanied by the peritectic reaction.

The experiments allowed the identification of the intermetallic compound / phase sub-layers, Figure 6.

The areas which contains the N^F- solution were identified in the case of the joint visible in Figure 6a.

The pure Al - areas resulting from the so-called "*mantis phenomenon*" revealed by Wołczyński et al. (2006b) (full consumption of the Al_3Ni compound by the Al_3Ni_2 – dominant phase) and described adequately by the reaction $2\,Al_3Ni \rightarrow Al_3Ni_2 + 3\,Al$ were also identified in the case of the current analysis, Figure 6b.

The suggested reaction occurs just after completion of the solidification. This is the result of the system tendency towards thermodynamic equilibrium (towards the formation

of all the phases visible in the Ni-Al phase diagram in sequence: Al_3Ni_2, AlNi, $NiAl$, Ni_3Al and finally towards the exclusive existence of the (Ni) solution).

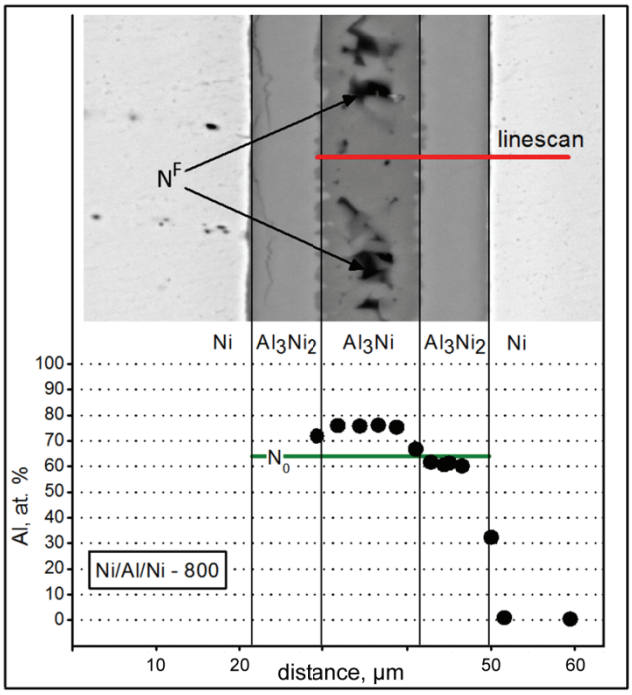

Figure 6a. The Ni / Al_3Ni_2 / Al_3Ni / Al_3Ni_2 / Ni Ni/Al/Ni joint morphology, ($T_R = 800$ °C), as observed at time $t < t^F$; the $\widehat{N}_0$ - parameter is estimated; time $t < t^F$ means that solidification was not yet completed and some areas of the N^F - solution exists inside the Al_3Ni sub-layer.

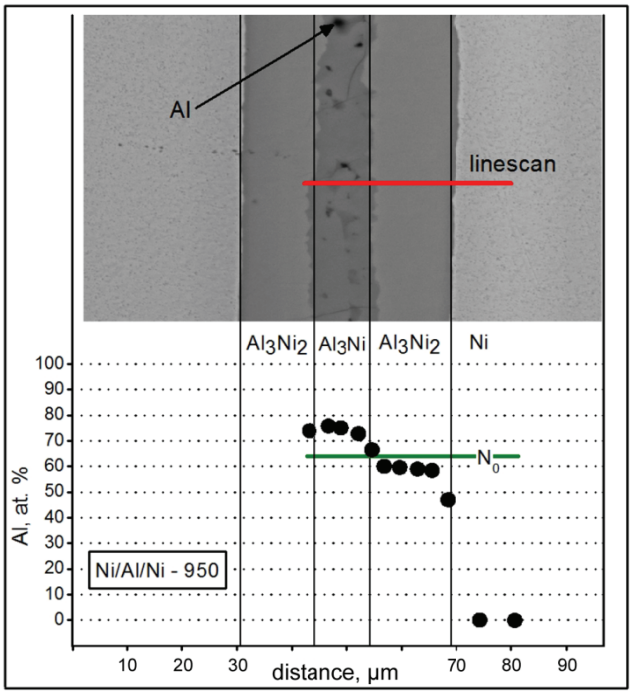

Figure 6b. The Ni / Al_3Ni_2 / Al_3Ni / Al_3Ni_2 / Ni Ni/Al/Ni joint morphology, ($T_R = 950$ °C), as observed at time $t > t_M$; the $\widehat{N}_0$ - parameter is estimated; time $t > t_M$ means that solidification was completed and the first solid / solid transformation occurred partially.

Table 1. Estimated values of the Al - solute content, $\widehat{N}_0$, within the Ni/Al/Ni joints formed at different temperatures T_R due to solidification arrested at time, t, with $t < t^F$.

T_R [^{0}C]	$\widehat{N}_0$ [at. %]
700	63.5
750	63.6
800	65.7
850	66.5
900	64.5
950	63.7
1000	62.5

In the case of the current analysis, the first step of this tendency is visible in Figure 6a (formation of the Al_3Ni phase and Al_3Ni_2 phase only).

The system begins to approach endeavor the thermodynamic equilibrium in the case of the joint shown in Figure 6b.

4. Meta-stable condition for the joint formation

N_0 - parameter localization on the liquidus line, as shown in Figure 3, indicates that the AlNi phase should be formed as the first sub-layer just at the substrate surface. Meanwhile, some experimental observations confirm the formation of the Al_3Ni_2 phase sub-layer but AlNi phase does not appear during the experiments, Figure 6.

It is evident that the solidification occurred under meta-stable conditions since the AlNi phase was not formed.

The transition of the system from stable conditions to meta-stable conditions can be justified by means of the Umeda-Okane-Kurz criterion, (Umeda et al. 1996).

The schematically drawn Ni-Al phase diagram for stable equilibrium is shown in Figure 7.

The characteristic $\bar{N}_0 = N_0$ - solute content is also situated on the phase diagram. The intersections of the N_0 - content with both meta-stable *solidus* lines defines T_f^* - temperatures of the s/l interface for both discussed phases.

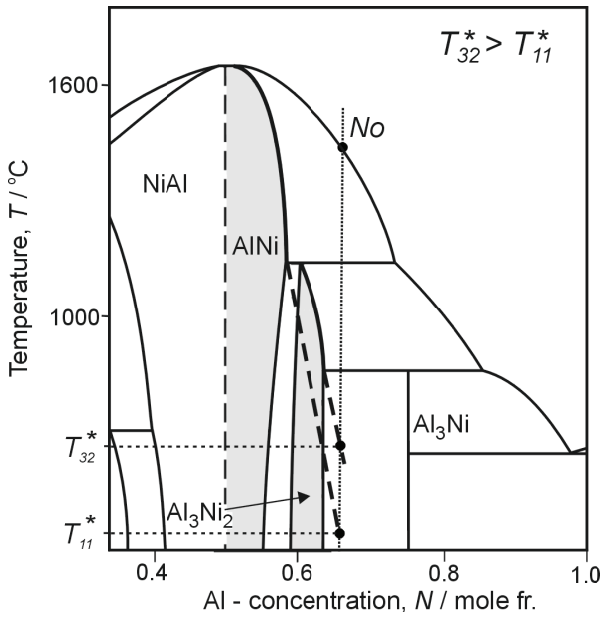

Figure 7. Application of the Umeda-Okane-Kurz criterion to the Ni-Al phase diagram for stable equilibrium. Two meta-stable solidus lines are added: first - for AlNi phase and second - for Al_3Ni_2 phase to explain a competition between the phases appearance during solidification.

According to the mentioned criterion, this phase is formed which manifests a higher temperature of its s/l interface during solidification. In the case of the Ni-Al system $T^*_{32} > T^*_{11}$ as visible and written in Figure 7. Therefore, the Al_3Ni_2 phase formation is selected by the system instead of expected AlNi phase formation. Temperature T^*_{11} results from the intersection of the meta-stable solidus line for the AlNi – phase (upper dashed line in Figure 7) and N_0 - solute concentration line (dotted line). Temperature T^*_{32} results from the intersection of the meta-stable solidus line for the Al_3Ni_2 – phase (lower dashed line in Figure 7.) and N_0 - solute concentration line (dotted line).

Additionally, some calculations made by means of the *Thermocalc Software* allowed some Ni-Al phase diagrams for meta-stable equilibrium to be reproduced as follows:

a/ for a dissolution, Figure 8,
b/ for a solidification resulting in formation of both observed phases, Figure 9.

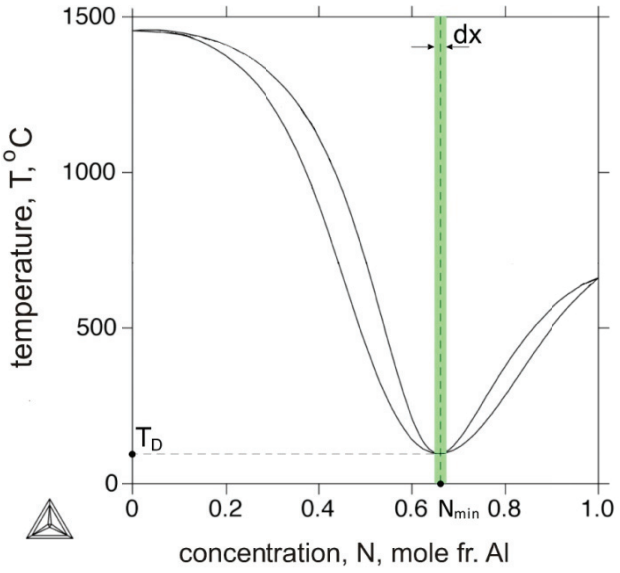

Figure 8. Ni-Al phase diagram for meta-stable equilibrium calculated for the solubility of Al (filler metal applied in the technology) in the Ni substrate. The upper line is the meta-stable liquidus and lower line is the meta-stable solidus.

The calculated phase diagram (meta-stable equilibrium) for the dissolution, Figure 8, manifests the minimum at the Al-solute concentration $N_{min} \approx 0.64$ [mole fr.].

It is evident that the N_{min} parameter value has the same meaning as the N_0 parameter value that represents the dissolution phenomenon in the model described by the scheme shown in Figure 1.

The minimum shown in Figure 8 defines the minimal temperature, T_D. At the T_D - temperature the dissolution (described in Figure 1) occurs as easily as possible. In other words, the appearance of minimum suggests that even at the T_D temperature the liquid solution can exist within the zone dx, Figure 1, under imposed meta-stable condition of the Ni/Al/Ni interconnection formation.

The phase diagram for dissolution is superposed onto the phase diagram for solidification in order to emphasize that both discussed phenomena occur cyclically, $N^F \rightarrow N_0$ (dissolution) and $N_0 \rightarrow N^F$ (solidification), Figure 9.

The dissolution path, $N^F \rightarrow N_0$, begins at *liquidus* line of the meta-stable equilibrium phase diagram calculated for solidification and is completed at the *liquidus* line minimum of the meta-stable equilibrium phase diagram calculated for dissolution (dashed green line), Figure 9.

The solidification path $N_0 \rightarrow N^F$, is situated on the *liquidus* line of the meta-stable equilibrium phase diagram calculated for the solidification, Figure 9.

The N^F – concentrations shown in Figures 1, 3 6a were measured by means of the scanning electron microscopy equipped with the EDAX energy dispersive X-ray (EDX) microanalyzer, Figure 10a, ($N^F_{exp.}$). Next, it was determined theoretically, Figure 10b, ($N^F_{theor.}$). Additionally, solute concentration in the zones ss and s is determined for a given T_R - isotherm.

The $N^F_{theor.}$ value was determined as the intersection of the T_T – isotherm and *liquidus* line of the phase diagram for meta-stable equilibrium, Figure 10b.

The ss - point results from the intersection of the T_R – isotherm and *solidus* line which is drawn in the meta-stable equilibrium phase diagram calculated for dissolution, while s - point is determined by *solidus* line of the meta-stable equilibrium phase diagram for solidification.

5. Concluding remarks

1/ Regardless of the real temperature, T_R, imposed in the technology, (Table 1), the beginning of the solidification path is always the same, and is equal to N_0.

2/ Regardless of the real temperature, T_R, the end of solidification path is always the same and is equal to N^F, which was confirmed experimentally, Figure 10a, and predicted theoretically, Figure 10b. Good agreement was obtained between both $N^F_{exp.}$ and $N^F_{theor.}$ parameters.

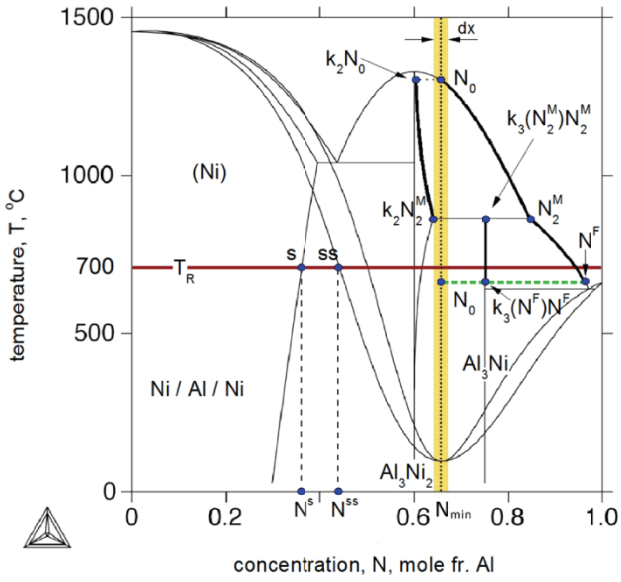

Figure 9. Superposition of the Ni-Al phase diagrams for meta-stable equilibrium calculated: a/ for the dissolution phenomenon discussed in Figure 8, and b/ for solidification resulting in the Ni/Al_3Ni_2/Al_3Ni/Al_3Ni_2/Ni joint formation.

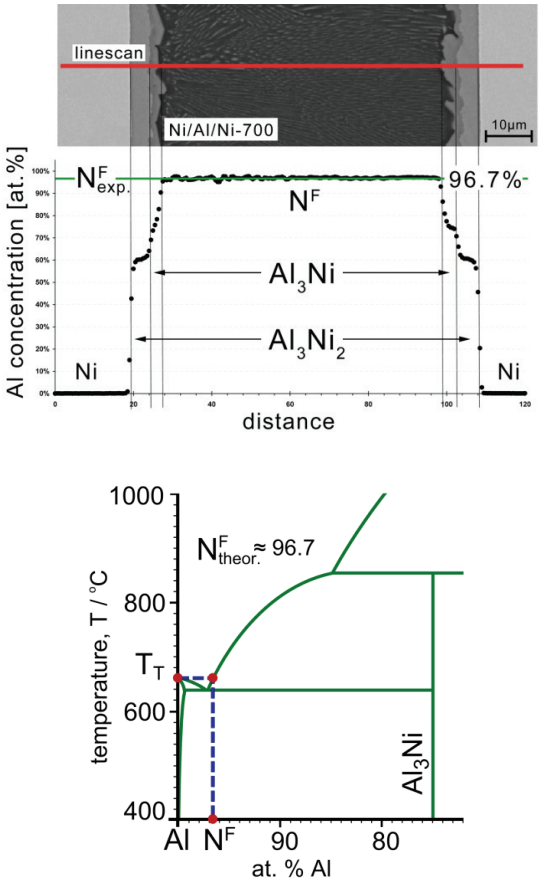

Figure 10. Method of determination of the N^F – parameter: a/ experimentally with Ni/Al/Ni-700 interconnection for which solidification was arrested and morphology frozen; b/ due to the Al-Ni meta-stable equilibrium phase diagram (T_T is the Al- melting point, N^F - is the solution of the Ni in the Al - filler metal, as shown in Figure 1).

3/ The N_0 – solute concentration is created within the zone dx as a result of dissolution, Figure 1-2.

4/ The N_0 – solute concentration is reproduced subsequently within the joint as an average solute concentration, Table 1.

5/ The N_0 – solute concentration created within the zone dx corresponds well to the N_{min} - solute concentration which is manifested by the meta-stable equilibrium phase diagram for dissolution, Figure 8. It is evident that both parameters are equal to each other: $N_0 \approx N_{min}$.

6/ The N_0 – solute concentration plays an essential role in the competition between stable and meta-stable formation of the interconnection, Figure 7.

7/ The N_0 – solute concentration located on the *liquidus* line, Figure 3, is treated as an initial condition for the differential equation which describes the solidification.

8/ According to the current model, creation of the zone dx, follows the reaction $N^F + Ni \rightarrow s(N^s) + ss(N^{ss}) + dx(N_0)$ as explained in Figure 11.

9/ According to the meta-stable equilibrium phase diagram, Figure 9, the first Al_3Ni_2 – intermetallic phase sub-layer (in sequence of appearance) is formed due to the phenomenon of partitioning along the solidification path $N_0 \Rightarrow N_2^M$ and diffusion into the solid (it is marked in Figure 11).

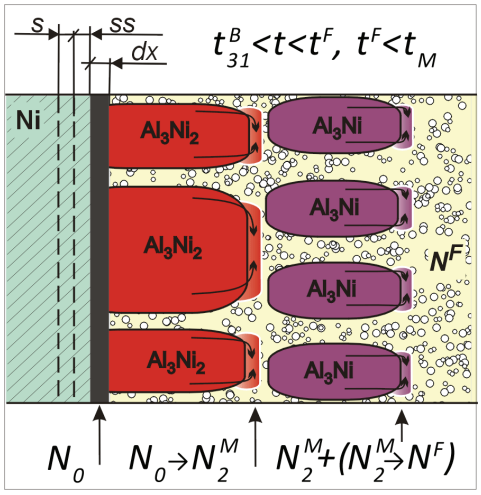

Figure 11. Localization of the zone dx, zone ss, and zone s within the Ni – substrate.

10/ According to the same phase diagram, Figure 9, the second Al_3Ni – intermetallic compound sub-layer is formed due to the interplay between the N_2^M - liquid and Al_3Ni_2 primary phase. Next, due to the partitioning along the solidification path $N_2^M \rightarrow N^F$ with diffusion into the solid (it is marked in Figure 11).

11/ Localizations of the N_2^M - liquid and Al_3Ni_2 primary phase in the growing joint suggests that the peritectic reaction (not peritectic transformation) takes place to form Al_3Ni – compound at the N_2^M – point, Figure 9 (according to the description by Phelan et al., 2006) (the occurrence of the peritectic reaction is marked in Figure 11).

12/ The Gibbs Phase Rule applied to the current model and experimental observations yields the Number of Degrees of Freedom $l = 0$, as required for the isothermal solidification imposed to the joint technology, $l = c - p + 1$. Thus $l = c - p + 1 = 0$ with $c \equiv Ni, Al$, and therefore $p = 3$,

13/ In fact, $p \equiv liquid(N_0)_{dx}$, Al_3Ni_2, Al_3Ni $= 3$, as it is justified by the current model and adequate experiments, Figures 6 and 10a.

14/ The model is a universal one and can be applied to other situations where the brazing is expected.

15/ It is suggested that brazing occurs in the case of massive rolls solidification, when the solid steel core interacts on the surrounding liquid cast iron added in the second step of the technology to improve the roll surface.

Acknowledgements

The financial support from the Polish Ministry of Science and Higher Education (MNiSW – Poland) under the contract: N R15 006 004 is gratefully acknowledged.

Nomenclature

c	number of elements which take part in a given reaction, (Gibbs Phase Rule),
dx	infinitesimal amount of the substrate melted due to the dissolution of the liquid Al solute, [mole fr.],
i	index of the range of solidification; $i = 1$ for the range $N_0 \Rightarrow N_1$; $i = 2$ for the range $N_1 \Rightarrow N_2$; $i = 3$ for the range $N_2 \Rightarrow N^F$, Figure 3,

k_i partition ratio varying with the concentration of solute in the liquid, $i = 1, \dots, n$, [mole fr./mole fr.],

k_i^0 first component of the partition ratio independent of any changes in the solute concentration along *liquidus* line, $i = 1, \dots, n$, [mole fr./mole fr.],

k_i^L second component of the partition ratio independent of any changes in the solute concentration along the *liquidus* line, $i = 1, \dots, n$, [mole fr./mole fr.],

L^0 amount of the liquid at the start of solidification, usually $L^0 = 1$, [dimensionless],

l Number of Degrees of Freedom for a given reaction, (Gibbs Phase Rule),

l_i^0 amount of the liquid at the beginning of a given range of solidification, i, $i = 1, \dots, n$, [mole fr.],

N_i^B solute redistribution after partitioning and back-diffusion, $i = 1, \dots, n$, Eq. (5P), (5C), [mole fr.],

N^F concentration of the Al - filler metal in its liquid solution at the T^T temperature, [mole fr.],

$N^F_{\text{exp.}}$ concentration of the filler metal in its liquid solution at the T^T temperature, determined experimentally, [mole fr.],

$N^F_{theor.}$ concentration of the filler metal in its liquid solution at the T^T temperature, determined theoretically, [mole fr.],

N_i^L solute concentration in the liquid, observed along the *liquidus* line for a given range of solidification, (local solidification path), $i = 1, \dots, n$, Eq. (1), Eq. (1P-3P), Eq. (1C-3C), [mole fr.],

N_i^S solute concentration at the solid / liquid interface, observed along the *solidus* line for a given range of solidification, (local solid/liquid interface path), $i = 1, \dots, n$, Eq. (4P), Eq. (4C), [mole fr.],

N_0 solute content at the beginning of solidification path (on *liquidus* line), [mole fr.], also is the Al - solute content within the zone dx, created at the substrate surface by the dissolution phenomenon,

$\widehat{N}_0$ average solute concentration measured across the formed multi-layer, [mole fr.],

$\overline{N_0}$ average solute concentration within the all investigated joints, [mole fr.],

N_1 solute concentration in the liquid at the first peritectic reaction (phase diagram for stable equilibrium), Figure 3, [mole fr.],

N_2 solute concentration in the liquid at the second peritectic reaction (phase diagram for stable equilibrium), Figure 3, [mole fr.],

N_2^M solute concentration in the liquid at the peritectic reaction (phase diagram for the meta-stable equilibrium), Figure 9, [mole fr.],

N_i solute concentration in the liquid at a given peritectic reaction (phase diagram for stable equilibrium), Figure 3, Eq. (2), $i = 1,2$, [mole fr.],

N_{i-1} solute concentration in the liquid at a given peritectic reaction, (for $i = 2,3$) or solute concentration at the beginning of solidification path (for $i = 1$), (phase diagram for stable equilibrium), Eq. (1), Figure 3, [mole fr.],

N^s solute concentration within the zone s, (Figure 9), [mole fr.],

N^{ss} solute concentration within the zone ss, (Figure 9), [mole fr.],

N_{min} solute concentration at the minimum of *liquidus* line, Figure 8, Figure 9, [mole fr.],

n number of ranges of solidification for a given solidification path, $n = 3$,

p number of phases which take part in a given reaction, (Gibbs Phase Rule),

s zone of saturation created in the substrate,

ss zone of super-saturation created in the substrate,

T_f^* temperature at the solid / liquid interface of a given phase / compound, f, $f \equiv AlNi, Al_3Ni_2, Al_3Ni$, (shortly, $f \equiv 11, 32, 31$) as it results from the intersection of a given meta-stable *solidus* line with the line which denotes N_0 concentration, [K],

T_{11}^* temperature of the AlNi phase solid /liquid interface, Figure 7, [K],

T_{32}^* temperature of the Al_3Ni_2 phase solid /liquid interface, Figure 7, [K],

T_D temperature at which the minimum of *liquidus* line appears in the phase diagram for meta-stable equilibrium, Figure 8, [K],

T_R real temperature of bonding (temperature of the interconnection formation), [K],

T^T melting temperature of the Al - filler metal, [K],

t^K time of the solidification progress, Figure 5a, [s],

t^F time at which solidification is completed, Figure 5b, Figure 11, [s],

t time, [s],

t_M time of the beginning of the first solid / solid transformation, Figure 11, [s],

t_{31}^B time of the birth of the Al_3Ni phase within the Ni/Al/Ni interconnection, Figure 11, [s],

X^0 amount of the solid at a given stage (progress) of solidification when the process is arrested and morphology frozen (calculated for a total system along a global solidification path) [dimensionless],

x current amount of the solid, [dimensionless],

x_i amount of the primary phase which takes part in a given peritectic reaction at the $i-th$ range of solidification, $i = 1, \dots, n$, [dimensionless],

x_i^0 amount of the solid at a given stage (progress) of solidification when the process is arrested and morphology frozen, (calculated for a given $i-th$ range of solidification along a local solidification path), [dimensionless],

x_i^{max} sum of amounts of both primary phase remaining after peritectic reaction and peritectic phase resulting from the peritectic reaction for a given solidification range, $i = 1, \dots, n$, [dimensionless],

x_i^{min} amount of the primary phase remaining after the peritectic reaction for a given solidification range, $i = 1, \dots, n$, [dimensionless];

$x_i^{max} - x_i^{min}$ denotes the amount of peritectic reaction product obtained for a given solidification range, $i = 1, \dots, n$, [dimensionless]; a peritectic reaction which occurs at the N_i solute concentration (on *liquidus*) is treated as belonging to the $i-th$ solidification range, (phase diagram for the stable equilibrium),

α_i^D back-diffusion parameter for both partitioning and redistribution, $i = 1, \dots, n$, [dimensionless],

β_i^{ex} redistribution extent coefficient, $i = 1, \dots, n$, (defined in detail by Wołczyński et al. 2006a), [dimensionless],

β_i^{in} redistribution intensity coefficient, $i = 1, \dots, n$, (defined in details by Wołczyński et al. 2006a), [dimensionless],

λ_1^F thickness of the Al_3Ni_2 phase sub-layer within the interconnection formed at time t^F, Figure 5, [μm],

λ_2^F half the thickness of the Al_3Ni phase sub-layer within the interconnection formed at time t^F, Figure 5, [μm],

λ_1^K thickness of the Al_3Ni_2 phase sub-layer within the interconnection formed at time t^K, Figure 5, [μm],

λ_2^K half the thickness of the Al_3Ni phase sub-layer within the interconnection formed at time t^K, Figure 5, [μm].

Appendix

The following mathematical formalism is applied for:

1/ formation of the intermetallic phase

The solute concentration in the liquid, changes during precipitation of primary phases along a given local solidification path, i, in accordance with the relationship:

$$N_i^L(x;\alpha_i^D, l_i^0, N_{i-1}, k_i^0) = N_{i-1}\left[(l_i^0 + \alpha_i^D\, k_i^0\, x - x)/l_i^0\right]^{\frac{k_i^0-1}{1-\alpha_i^D k_i^0}} \quad (1P)$$

The Eq. (1P) is the solution to differential equation:

$$dN_i^L/dx = (1-k_i^0)\, N_i^L/(l_i^0 + \alpha_i^D\, k_i^0\, x - x) \quad (2P)$$

with the initial condition:

$$N_i^L(0;\alpha_i^D, l_i^0, N_{i-1}, k_i^0) = N_{i-1} \quad (3P)$$

The phenomenon of partitioning results in the formation of the solid / liquid interfaces, and "history" of the solute concentration at the existed interfaces are given as:

$$N_i^S(x;\alpha_i^D, l_i^0, N_{i-1}, k_i^0) = k_i^0\, N_i^L(x;\alpha_i^D, l_i^0, N_{i-1}, k_i^0) \quad (4P)$$

The phenomenon of back-diffusion superposes solute partitioning.

The superposition of both phenomena results in the solute redistribution, which is a function of the solute concentration at formerly existing solid / liquid interfaces.

$$N_i^B\left(x; x_i^0, \alpha_i^D, l_i^0, N_{i-1}, k_i^0\right) = N_i^S\left(x;\alpha_i^D, l_i^0, N_{i-1}, k_i^0\right) \times \left[1 + \beta_i^{ex}\left(x; x_i^0, l_i^0, k_i^0\right)\beta_i^{in}\left(x_i^0, \alpha_i^D, l_i^0, k_i^0\right)\right] \quad (5P)$$

2/ formation of the intermetallic compound

The solute concentration in the liquid changes during precipitation of primary phases along a given solidification path, i, in accordance with the following relationship:

$$N_i^L(x;\alpha_i^D, l_i^0, N_{i-1}, k_i) = [N_{i-1}/(1-k_i^0)] \times \left\{k_i^L + (1-k_i^0-k_i^L)[(l_i^0 + \alpha_i^D\, k_i^0\, x - x)/l_i^0]^{\frac{k_i^0-1}{1-\alpha_i^D k_i^0}}\right\} \quad (1C)$$

Eq. (1C) is the solution to differential equation for solidification/micro-segregation:

$$dN_i^L/dx = \left[(1-k_i^0)\, N_i^L - k_i^L\, N_{i-1}\right]/(l_i^0 + \alpha_i^D\, k_i^0\, x - x) \quad (2C)$$

with the initial condition:

$$N_i^L(0;\alpha_i^D, l_i^0, N_{i-1}, k_i^0, k_i^L) = N_{i-1} \quad (3C)$$

The "history" of solute concentration, at the appearing interfaces is described as follows:

$$N_i^S(x;\alpha_i^D, l_i^0, N_{i-1}, k_i) = k_i^0\, N_i^L(x;\alpha_i^D, l_i^0, N_{i-1}, k_i) + k_i^L\, N_{i-1} \quad (4C)$$

Consequently, the solute redistribution after partitioning and back-diffusion is given by:

$$N_i^B(x; x_i^0, \alpha_i^D, l_i^0, N_{i-1}, k_i) = N_i^S(x;\alpha_i^D, l_i^0, N_{i-1}, k_i) \times \left[1 + \beta_i^{ex}(x; x_i^0, l_i^0, k_i)\,\beta_i^{in}(x_i^0, \alpha_i^D, l_i^0, k_i)\right] \quad (5C)$$

All the relationships are formulated with:

$$l_i^0 = \begin{cases} L^0, & i = 1; \\ L^0 - \sum_{j=1}^{i-1} x_j^{max}, & i = 2, \dots, n; \end{cases} \quad (1A)$$

$$x_i^0 = \begin{cases} X^0, & i = 1; \\ X^0 - \sum_{j=1}^{i-1} x_j^{max}, & i = 2, \dots, n; \end{cases} \quad (2A)$$

Additionally, the coefficient of the redistribution extent $\beta_i^{ex}(x; x_i^0, l_i^0, k_i)$ is the solution to the following equation:

$$(1+\beta_i^{ex})\, N_i^S(x; 1, l_i^0, N_{i-1}, k_i) = N_i^S(x_i^0; 1, l_i^0, N_{i-1}, k_i) \quad (3A)$$

Moreover, the definition of the coefficient of the redistribution intensity was also formulated.

The $\beta_i^{in}(x_i^0; \alpha_i^D, l_i^0, k_i)$ – coefficient of the redistribution intensity is a result of the solution to the equation:

$$\int_0^{x_i^0}\left[1 + \beta_i^{in}\,\beta_i^{ex}(x; x_i^0, l_i^0, k_i)\right]\, N_i^S(x;\alpha_i^D, l_i^0, k_i)\, dx = l_i^0\, N_{i-1} - (l_i^0 - x_i^0)\, N_i^L(x_i^0;\alpha_i^D, l_i^0, N_{i-1}, k_i) \quad (4A)$$

References

Chuang, Y.K., Reinisch, D. & Schwerdtfeger, K. (1975). Kinetics of Diffusion Controlled Peritectic Reaction During Solidification of Iron-Carbon Alloys, *Metallurgical Transactions, 6(A), 235-238.*

Kloch, J., Guzik, E., Janczak-Rusch, J., Kopyciński, D., Rütti, T., Kim, J., Lee, H.M. & Wołczyński, W. (2005). Morphological Characteristics of the Multi-layer/Substrate Systems, *Proceedings of the 9th European Congress on Stereology and Image Analysis, Zakopane (Poland), 375-382.*

Jacobson, D.M. & Humpston, G. (1992). Diffusion Soldering, *Soldering & Surface Mount Technology,10, 27-32.*

Tuah-Poku, I., Dollar, M. & Massalski, T. (1988). A Study of the Transient Liquid Phase Bonding Process Applied to a Ag/Cu/Ag Sandwich Joint, *Metallurgical Transactions, 19A, 675-686.*

Umeda, T., Okane, T. & Kurz,W. (1996), Phase Selection during Solidification of Peritectic Alloys, *Acta Materialia, 44, 4209-4216.*

Wołczyński, W., Guzik, E., Kopyciński, D., Himemiya, T. & Janczak-Rusch, J. (2006a). Mass Transport during Diffusion Soldering or Brazing at the Constant Temperature, *Proceedings of the 13th International Heat Transfer Conference – Sydney (Australia), ed. Begell House, eds. G.de Vahl Davis & E.Leonardi, CD, MST-11, 12 pages.*

Wołczyński, W., Kloch, J., Janczak-Rusch, J., Kurzydłowski, K. & Okane, T. (2006b). Segregation Profiles in Diffusion Soldered Ni/Al/Ni Interconnections, *Materials Science Forum, 508, 385-392.*

Phelan, D., Reid, M. & Dippenaar, R. (2006), Kinetics of the Peritectic Phase Transformation: In-situ Measurements and Phase Field Modelling, *Metallurgical and Materials Transactions, 37A, 985-994.*